

# Synthesis and *In vitro* Evaluation of Electrodeposited Barium Titanate Coating on Ti6Al4V

Shahram Rahmati, Mohammad Basir Basiriani<sup>1</sup>, Mohammad Rafienia<sup>2</sup>, Jaber Yaghini<sup>3</sup>, Keyvan Raeisi<sup>1</sup>

Department of Biomaterials, Nanotechnology and Tissue Engineering, School of Advanced Medical Technologies, Isfahan University of Medical Sciences, <sup>2</sup>Biosensor Research Center, Isfahan University of Medical Sciences, <sup>3</sup>Department of Periodontology, School of Dentistry, Dental Implant Research Center, Isfahan University of Medical Sciences, Isfahan, 81744176, <sup>1</sup>Department of Materials Engineering, Isfahan University of Technology, Isfahan, 8415683111, Iran

Submission: 04-02-2016

Accepted: 08-03-2016

## ABSTRACT

Osseointegration has been the concern of implantology for many years. Researchers have used various ceramic coatings for this purpose; however, piezoelectric ceramics (e.g., barium titanate [BTO]) are a novel field of interest. In this regard, BTO (BaTiO<sub>3</sub>) coating was fabricated by electrophoretic deposition on Ti6Al4V medical alloy, using sol-gel-synthesized nanometer BTO powder. Structure and morphologies were studied using X-ray diffraction and scanning electron microscopy (SEM), respectively. Bioactivity response of coated samples was evaluated by SEM and inductively coupled plasma (ICP) analysis after immersion in simulated body fluid (SBF). Cell compatibility was also studied via MTT assay and SEM imaging. Results showed homogenous coating with cubic structure and crystallite size of about 41 nm. SEM images indicated apatite formation on the coating after 7 days of SBF immersion, and ICP analysis approved ions concentration decrement in SBF. Cells showed flattened morphology in intimate contact with coating after 7 days of culture. Altogether, coated samples demonstrated appropriate bioactivity and biocompatibility.

**Key words:** Barium titanate, bioactivity, cytotoxicity, electrophoretic deposition, sol-gel

## INTRODUCTION

Healing process in the implants is based on osseointegration that was defined as direct contact between bone and implant without microscopic deflection by Berglundh *et al.*<sup>[1]</sup> Minimum trauma in surgery, initial stability, and prevention of infection and micromotion are fundamental requirements for osseointegration.<sup>[1]</sup> Osseointegration and bone response in the case of formation rate, quantity, and quality of the new bone depend on implant properties.<sup>[2]</sup> Studies have shown that faster bone modeling can fix implant tightly and prevent fibrous layer formation on the surface of implant.<sup>[3]</sup> Various techniques have been used to improve bone and implant surface connection with the goal of faster integration, bone remodeling, and more implant stability during healing time so that earlier loading could be applied.<sup>[2]</sup>

Implant properties such as surface chemistry, electrical charge, surface topography, and porosity could affect bone

response at *in vivo* conditions.<sup>[4]</sup> Titanium and its alloys are the most commercial alloys used for implants due to their mechanical properties, corrosion resistance, and biocompatibility.<sup>[5,6]</sup> Different methods have been used to improve implant properties and its integration, such as different coatings like titania, calcium phosphate, or hydroxyapatite, as well as surface roughening or chemical modifications on the implant surface.<sup>[6-9]</sup> However, another concept in this case are piezoelectric materials. They could be useful because of bone intrinsic piezoelectricity.<sup>[10,11]</sup>

Barium titanate (BTO), due to its well-known piezoelectric properties, is one of the electroactive ceramics that has the

This is an open access article distributed under the terms of the Creative Commons Attribution-NonCommercial-ShareAlike 3.0 License, which allows others to remix, tweak, and build upon the work non-commercially, as long as the author is credited and the new creations are licensed under the identical terms.

**For reprints contact:** reprints@medknow.com

**Address for correspondence:**  
Dr. Mohammad Rafienia, Biosensor Research Center, Isfahan University of Medical Sciences, P. O. Box 64716, Isfahan, Iran.  
E-mail: m\_rafienia@med.mui.ac.ir

**How to cite this article:** Rahmati S, Basiriani MB, Rafienia M, Yaghini J, Raeisi K. Synthesis and *In vitro* Evaluation of Electrodeposited Barium Titanate Coating on Ti6Al4V. J Med Sign Sence 2016;6:106-11.

capability of being used as a bioceramic.<sup>[12,13]</sup> Among various coating methods, electrophoretic deposition (EPD) is a simple and inexpensive method that has interested many researchers in recent years for coating of diverse bioceramics such as hydroxyapatite,<sup>[14]</sup> bioglass,<sup>[15]</sup> and forsterite.<sup>[16]</sup> EPD is an easy, fast, and inexpensive method that provides homogeneous high purity coatings. Furthermore, this method allows coating thickness modification via its various processing parameters.<sup>[17]</sup> Many researchers have studied EPD process for BTO<sup>[18-20]</sup> but no biomedical evaluation has been reported.

In this study, BTO was introduced as a novel bioceramic coating. BTO electrophoretically was coated on Ti6Al4V medical alloy and its bioactivity and cell compatibility were studied.

## MATERIALS AND METHODS

### Barium Titanate Powder Synthesis

BTO was synthesized via sol-gel method based on Kuwabara and Miki experiences.<sup>[21]</sup> Equimolar amounts of barium diethoxide ( $\text{Ba}(\text{OC}_2\text{H}_5)_2$ , Alfa Aesar, USA), and titanium tetraisopropoxide ( $\text{Ti}(\text{OC}_3\text{H}_7)_4$ , Alfa Aesar, USA) were dissolved in ethylene glycol monomethyl ether (EGMME:  $\text{CH}_3\text{OC}_2\text{H}_4\text{OH}$ , Merck, Germany) to prepare precursor solution with the concentration of 0.25 M under dry argon atmosphere. The solution was hydrolyzed by adding water and EGMME (with a volume ratio of 1:1) at  $-17^\circ\text{C}$  for 20 min. After aging for 24 h, the obtained gel was dried at  $90^\circ\text{C}$  and heat-treated at  $800^\circ\text{C}$  for 1 h.

### Electrophoretic Deposition

A mixture of EGMME and acetylacetone (Acac:  $\text{CH}_3\text{COCH}_2\text{COCH}_3$ , Merck, Germany), with a volume ratio of 9:1, was used as electrophoretic medium. BTO particles were added to the solution with a concentration of 0.2 M and agitated ultrasonically to achieve a stable suspension. Two Ti6Al4V (ASTM grade 5, Galimplant S.L., Spain) plates of  $1\text{ cm} \times 1\text{ cm}$  were used as electrodes with a distance of 2 cm. The specimens were prepared by grinding with silicon carbide abrasive paper up to 600 grits. A DC voltage of 60 V was applied for 3 min. Coatings were dried in the air at  $90^\circ\text{C}$  and sintered at  $800^\circ\text{C}$  for 1 h.

### Structural Characterization

X-ray diffraction (XRD, Philips X'Pert-MPD System, The Netherlands) with  $\text{CuK}_\alpha$  beam ( $\lambda = 0.1543\text{ nm}$ ) was used for structure analysis in according to Joint Committee on Powder Diffraction Standards (JCPDS) standard cards. The crystallite size of synthesized powder and coating was determined using the Scherrer equation (Eq. 1):

$$t = \frac{k\lambda}{\beta \cos\theta} \quad (1)$$

Where  $\beta$  is the width of peak in the middle of its height,  $\lambda$  is the wavelength (0.154 nm),  $\theta$  is the Bragg angle,  $k$  is a constant (0.9), and  $t$  is the apparent crystallite size.

### Size and Morphologies

The powder particle size distribution was evaluated by dynamic light scattering (DLS, Malvern ZEN3600, UK). The morphology of coatings was investigated by scanning electron microscopy (SEM, Philips XL30, The Netherlands) after gold coating (about several nanometers thick) using a sputter coater (Bal-Tec, SCD 005, USA) to create surface conductivity.

### Bioactivity Evaluation

Bioactivity of BTO coatings was evaluated by immersing in simulated body fluid (SBF) prepared using Kokubo method.<sup>[22]</sup> After immersion for 28 days, specimens' surface morphology and element analysis was studied using an SEM equipped with energy dispersive X-ray spectroscopy (EDS, SeronAIS-2100, Korea) system. Ions concentration changes also evaluated by means of inductively coupled plasma (ICP, Optima 7300DV, USA) analysis for days of 3, 7, 14, and 28.

### Cell Culture

MG-63 cell line cells were cultured in a Dulbecco's modified Eagle's medium (DMEM, Bio-Idea, Iran) containing 10% fetal bovine serum (FBS, Bio-Idea, Iran) and 1% Penicillin/streptomycin (Pen/strep, Bio-Idea, Iran) for several passages to reach a stable phenotype. About 10,000 cells were seeded on each sample and were incubated in  $37^\circ\text{C}$  and 5%  $\text{CO}_2$  atmosphere. After 1 and 7 days, samples were washed with phosphate-buffered saline (PBS, Bio-Idea, Iran) to eliminate unattached cells and fixed in 2% glutaraldehyde for 30 min at room temperature. After several dehydrations in ethanol (30 min in 50%, 70%, 80%, 90%, and 100% ethanol, subsequently), SEM (Philips XL30, The Netherlands) was used to study cells morphology on the surface.

### MTT Assay

For 3-(4,5-dimethylthiazol-2-yl)-2,5-diphenyltetrazolium (MTT) assay about  $1 \times 10^4$  cells were seeded on  $1\text{ cm} \times 1\text{ cm}$  coated samples and were incubated for 1, 4, and 7 days in a 24 well plate (three samples for each day). Polystyrene plate (Biofil, China) was also used as control. At specific intervals after the removal of culture medium, 700  $\mu\text{l}$  DMEM and 70  $\mu\text{l}$  (MTT, 5 mg/ml in PBS) were added to each well, and they were incubated for 3 h. Afterward, the medium was removed, and 700  $\mu\text{l}$  dimethyl sulfoxide (DMSO, Sigma, UK) was added to each well. The samples were incubated for 1 h. DMSO was removed and added to three wells of a 96 well-plate, and the absorbance was read using an automated plate reader (Microplate Reader Model 1680,

Bio-Rad, USA) at 540 nm, subsequently. The average value and standard deviation of optical density were calculated and reported.  $P < 0.05$  was considered statistically significant in statistical analyses using ANOVA.

## RESULTS AND DISCUSSIONS

### Phase Structure Analysis

Figure 1 shows XRD patterns of the synthesized powder and coating. According to the standard card of BTO (JCPDS#01-075-0212), both of them have cubic perovskite structure. Patterns have no lack of peaks and no additional peaks in comparison to standard. Coating shows sharper and higher peaks especially in high angles that reveals higher crystallinity. Calculated crystallite size of the powder was about 25 nm while it was 41 nm for the coating. Furthermore, small peak transition to lower angles could be seen in almost all peaks that show more interplanar distance. All are results of coating further sintering process that eased diffusion and made structure more crystalline.

### Particle Size Evaluation

DLS analysis of particles size is shown in Figure 2. As it can be seen, particles are in the range of 40–110 nm with one peak around 70 nm. In comparison to XRD

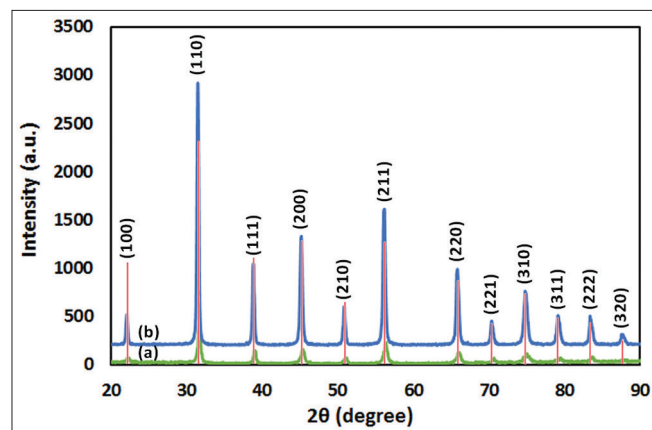


**Figure 1:** X-ray diffraction patterns of barium titanate synthesized powder (a) and coating (b). Red bars are JCPDS #01-075-0212 standard

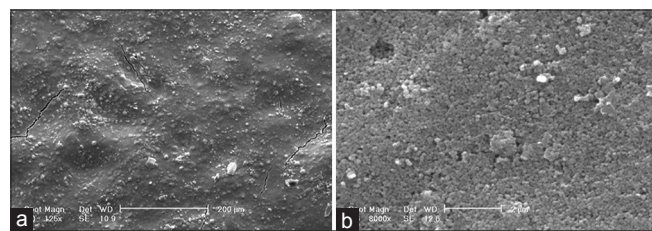


**Figure 3:** Scanning electron microscopy micrographs of barium titanate coating deposited by electrophoretic deposition under 60 V/3 min. (a) 125X, (b) 8000X

results, it seems that each particle consists of a few numbers crystallites. Li *et al.*<sup>[23]</sup> reached to an average size of ~10 nm via a similar synthesis method for both crystallite and particle sizes. This difference may relate to better powder dispersion and their colder hydrolyzing temperature ( $-20^{\circ}\text{C}$ ) that provided higher activation free energy for nucleation.

### Coating Morphology

Figure 3 demonstrates SEM images of the samples after sintering. Particles agglomeration is obvious with signs of substrate roughness. Micro-holes that are the cause of electrolyte evaporation during drying and some micro-cracks were inevitable. Notwithstanding the presence of these defects, coatings have had sufficient qualitative strength and adhesion to substrate.

### Bioactivity Evaluation

*In vitro* biomineralization of the coated samples after 4 weeks of immersion in SBF is shown in Figure 4. Apatite nuclei are appearing on the surface. Globular precipitates growth and conjugation occurred, and new nuclei are obvious on the surface of older ones after 28 days. According to scale bar, size of each globe is about  $10\ \mu\text{m}$ .

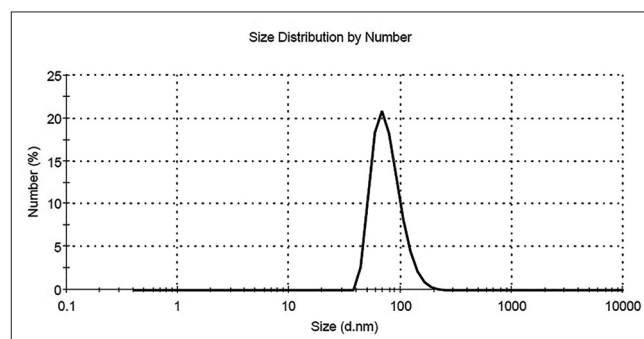


**Figure 2:** Particle size distribution of synthesized nanoparticles

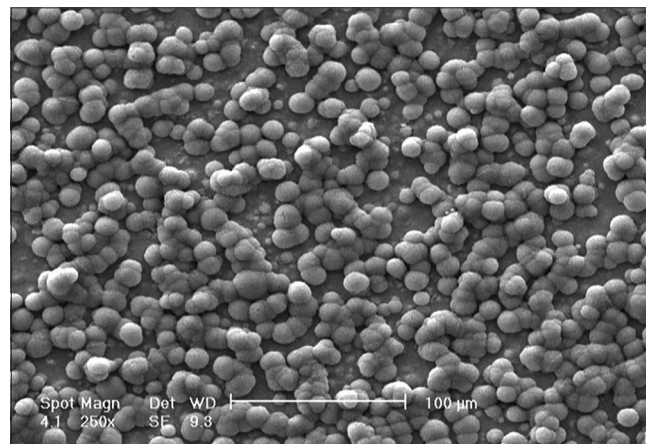


**Figure 4:** Scanning electron microscopy micrograph of barium titanate surface immersed in simulated body fluid after 28 days

Lin *et al.*<sup>[24]</sup> have reported ball-like calcium phosphate film on the surface of BTO/TiO<sub>2</sub> after 21 days immersion in SBF, but with the size of about 3  $\mu\text{m}$ . This size was less than 1  $\mu\text{m}$  in Zarkoob *et al.*<sup>[25]</sup> study on BTO/hydroxyapatite. Also in those studies precipitates have covered the surface completely. It seems that there is no appropriate compatibility between BTO and formed apatites, so newer precipitates prefer to form on the surface of older ones instead of BTO surface. This leads to bigger apatite globes versus BTO regions that not covered with precipitates.

EDS result on the sample [Figure 5] qualified precipitates apatite chemistry while it is well known that using standard less EDS analysis do not have sufficient quantitative accuracy to determine the formula of a compound.<sup>[26]</sup>

SBF ions concentration during 4 weeks of bioactivity test is shown in Figure 6. Calcium and phosphate ions decreased with an increasing rate, because of growing apatites are more suitable substrates for new apatite nucleation and make precipitation faster. The difference in Ca<sup>2+</sup> and PO<sub>4</sub><sup>3-</sup> losing amount is related to apatite stoichiometry (Ca<sub>10</sub>(PO<sub>4</sub>)<sub>6</sub>(OH)<sub>2</sub>) that needs Ca<sup>2+</sup> about 2 times more than PO<sub>4</sub><sup>3-</sup>. On the other

hand, it could be seen that Ba<sup>2+</sup> leached from coating to the solution, as also have seen previously in nanometric BTO.<sup>[27]</sup> Nevertheless, apatite precipitates slow down the releasing rate of Ba<sup>2+</sup> ions by covering the surface along with time.

## Cell Culture

The morphology of MG-63 cells cultured on BTO-coated samples was examined using SEM. Some of the images obtained of cells cultured after 1 and 7 days are shown in Figure 7. After 24 h, the appearance of lamellipodia demonstrates cells migration on the surface<sup>[28]</sup> to reach to an appropriate distribution. On the 7<sup>th</sup> day, cells completely covered the surface (even over micro-cracks) and showed good attachment to each other and BTO surface.

## MTT Assay

Figure 8 shows MTT assay results comparing the samples and control. BTO had no statistically significant changes during 7 days while control showed cell proliferation. However, this difference could not simply consider as a sign

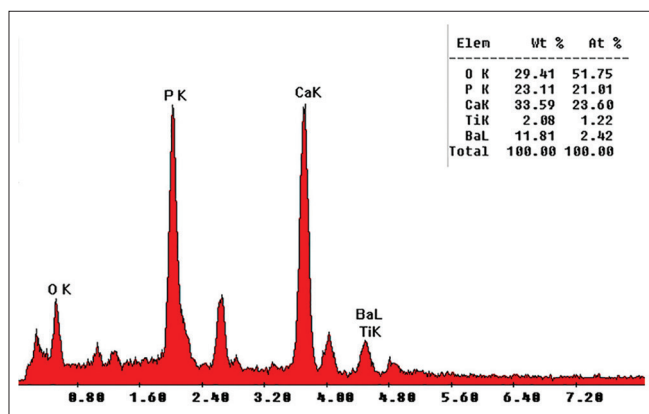


**Figure 5:** Energy dispersive X-ray spectroscopy spectra of apatite nuclei after 28 days of immersion in simulated body fluid

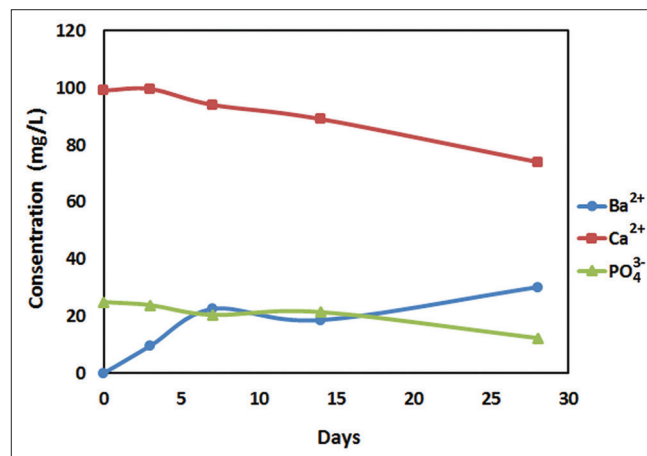


**Figure 6:** Simulated body fluid ions concentration changing in the presence of barium titanate coated samples during 4 weeks

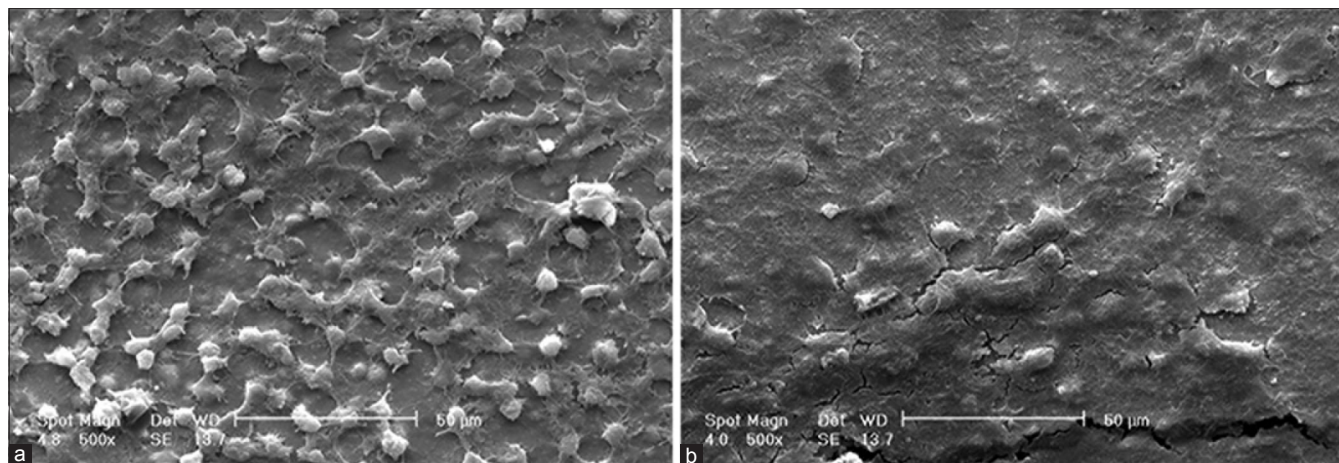


**Figure 7:** MG-63 cells morphology after 1 (a) and 7 (b) days of culture on the surface of barium titanate coating

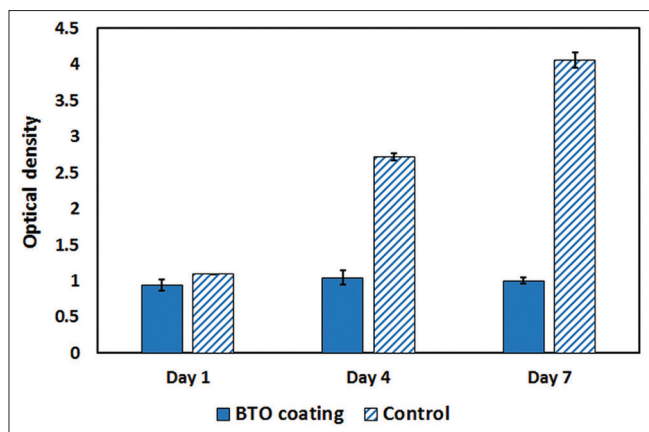


**Figure 8:** MTT assay results for barium titanate coating and control in 1, 4, and 7 days after culture

of cytotoxicity since cells were seen in SEM images flattened and attached to the surface.

One probable reason may be  $Ba^{2+}$  ions leaching from ceramic as we have discussed in section “Bioactivity Evaluation.” Studies that have investigated composites involving BTO particles, with adequate MTT results<sup>[28,29]</sup> have had micrometer size BTO particles. According to few studies, heat treatment in higher temperatures could decrease  $Ba^{2+}$  ions leaching by means of two parameters. High temperatures increase particle sizes and consequently decrease surface/volume ratio that leads to lower ion leaching.<sup>[30]</sup> However, by increasing particle size, BTO curie temperature increases and make tetragonal BTO as the stable phase in room temperature.<sup>[31]</sup> Cubic BTO has exhibited  $Ba^{2+}$  leaching about 3.6 times more than tetragonal BTO because of their differences in crystal structures and the amount of lattice defects contained.<sup>[30]</sup> Hence, it seems that further sintering processes could be useful to make micrometer size particles and eliminate ions leaching.

Furthermore, in some special circumstances, cultured fibroblasts on the piezoelectric scaffolds have shown that prefer to migrate, adhere, and secrete extracellular matrix,<sup>[32]</sup> means may be bioactivity of BTO leads to lower cell number and higher protein deposition, that needs a series of protein analyses for approval.

## CONCLUSION

Ti6Al4V coated samples with BTO were fabricated by EPD using synthesized nanometer BTO powders followed by sintering at 800°C. Morphological studies showed homogenous coating with signs of EPD medium evaporation. Bioactivity of the coated specimens was studied in SBF at 37°C endorsed apatite formation on the surface. Cell seeding also showed good attachment to the surface but MTT assay resulting in lack of proliferation that may be a result of ion leaching. Hence the results show capability of BTO coating to use as implant coating for *in vivo* applications.

## Acknowledgment

The authors would like to express their appreciation to the Iran National Science Foundation (INSF) for the financial support (Grant no. 91002863).

## Financial Support and Sponsorship

Iran National Science Foundation (INSF) (Grant No. 91002863).

## Conflicts of Interest

There are no conflicts of interest.

## REFERENCES

- Berglundh T, Abrahamsson I, Lang NP, Lindhe J. *De novo* alveolar bone formation adjacent to endosseous implants. *Clin Oral Implants Res* 2003;14:251-62.
- Novaes AB Jr, de Souza SL, de Barros RR, Pereira KK, Iezzi G, Piattelli A. Influence of implant surfaces on osseointegration. *Braz Dent J* 2010;21:471-81.
- Elmengaard B, Bechtold JE, Søballe K. *In vivo* study of the effect of RGD treatment on bone ongrowth on press-fit titanium alloy implants. *Biomaterials* 2005;26:3521-6.
- Ferris DM, Moodie GD, Dimond PM, Gioranni CW, Ehrlich MG, Valentini RF. RGD-coated titanium implants stimulate increased bone formation *in vivo*. *Biomaterials* 1999;20:2323-31.
- Sennerby L, Dasmah A, Larsson B, Iverhed M. Bone tissue responses to surface-modified zirconia implants: A histomorphometric and removal torque study in the rabbit. *Clin Implant Dent Relat Res* 2005;7 Suppl 1:S13-20.
- Giavresi G, Ambrosio L, Battiston GA, Casellato U, Gerbasì R, Finia M, et al. Histomorphometric, ultrastructural and microhardness evaluation of the osseointegration of a nanostructured titanium oxide coating by metal-organic chemical vapour deposition: An *in vivo* study. *Biomaterials* 2004;25:5583-91.
- Klokkevold PR, Nishimura RD, Adachi M, Caputo A. Osseointegration enhanced by chemical etching of the titanium surface. A torque removal study in the rabbit. *Clin Oral Implants Res* 1997;8:442-7.
- Balla VK, Banerjee S, Bose S, Bandyopadhyay A. Direct laser processing of a tantalum coating on titanium for bone replacement structures. *Acta Biomater* 2010;6:2329-34.
- Le Guéhennec L, Soueidan A, Layrolle P, Amouriq Y. Surface treatments of titanium dental implants for rapid osseointegration. *Dent Mater* 2007;23:844-54.
- Fukada E, Yasuda I. On the piezoelectric effect of bone. *J Phys Soc Jpn* 1957;12:1158.
- Marino A, Becker RO. Piezoelectric effect and growth control in bone. *Nature* 1970;228:473-4.
- Feng J, Yuan H, Zhang X. Promotion of osteogenesis by a piezoelectric biological ceramic. *Biomaterials* 1997;18:1531-4.
- Park JB, von Recum AF, Kenner GH, Kelly BJ, Coffeen WW, Grether MF. Piezoelectric ceramic implants: A feasibility study. *J Biomed Mater Res* 1980;14:269-77.
- Kwok CT, Wong PK, Cheng FT, Man HC. Characterization and corrosion behavior of hydroxyapatite coatings on Ti6Al4V fabricated by electrophoretic deposition. *Appl Surf Sci* 2009; 255:6736-44.
- Rojaei R, Fathi MH, Raeissi K, Taherian MH. Electrophoretic deposition of bioactive glass nanopowders on magnesium based alloy for

- biomedical applications. *Ceram Int* 2014;40:7879-88.
16. Hosseini SN, Jazi HS, Fathi M. Novel electrophoretic deposited nanostructured forsterite coating on 316L stainless steel implants for biocompatibility improvement. *Mater Lett* 2015;143:16-9.
  17. Besra L, Liu M. A review on fundamentals and applications of electrophoretic deposition (EPD). *Progress in Materials Science* 2007;52:1-61.
  18. Raju K, Yoon DH. Electrophoretic deposition of BaTiO<sub>3</sub> in an aqueous suspension using asymmetric alternating current. *Mater Lett* 2013;110:188-90.
  19. Wu YJ, Li J, Koga T, Kuwabara M. Low-temperature synthesis of barium titanate thin films by nanoparticles electrophoretic deposition. *J Electroceramics* 2008;21:189-92.
  20. Dogan A, Gunkaya G, Suvaci E, Niederberger M. Electrophoretic deposition of nanocrystalline BaTiO<sub>3</sub> in ethanol medium. *Key Eng Mater* 2006;314:133-40.
  21. Kuwabara M, Miki K. Preparation of monolithic barium titanate xerogels by sol-gel processing and the dielectric properties of their sintered bodies. *Appl Phys Lett* 1995;66:1704-6.
  22. Kokubo T, Takadama H. How useful is SBF in predicting *in vivo* bone bioactivity? *Biomaterials* 2006;27:2907-15.
  23. Li J, Wu YJ, Tanaka H, Yamamoto T, Kuwabara M. Preparation of a monodispersed suspension of barium titanate nanoparticles and electrophoretic deposition of thin films. *J Am Ceram Soc* 2004;87:1578-81.
  24. Lin CM, Yen SK. Biocompatibility and Corrosion Behavior of BaTiO<sub>3</sub>/TiO<sub>2</sub> Double Layers by Electrochemical Synthesis. *Key Eng Mat* 2006;309-311:371-4.
  25. Zarkoob H, Ziaei-Rad S, Fathi M, Dadkhah H. Synthesis, Characterization and Bioactivity Evaluation of Porous Barium Titanate with Nanostructured Hydroxyapatite Coating for Biomedical Application. *Advanced Engineering Materials*. 2012;14:B332-B339.
  26. Newbury DE, Ritchie NW. Is scanning electron microscopy/energy dispersive X-ray spectrometry (SEM/EDS) quantitative? *Scanning* 2013;35:141-68.
  27. Yoon DH, Lee BI, Badheka P, Wang X. Barium ion leaching from barium titanate powder in water. *J Mater Sci Mater Electron* 2003;14:165-9.
  28. Baxter FR, Turner IG, Bowen CR, Gittings JP, Chaudhuri JB. An *in vitro* study of electrically active hydroxyapatite-barium titanate ceramics using Saos-2 cells. *J Mater Sci Mater Med* 2009;20:1697-708.
  29. Teixeira LN, Crippa GE, Trabuco AC, Gimenes R, Zaghe MA, Palioto DB, et al. *In vitro* biocompatibility of poly(vinylidene fluoride-trifluoroethylene)/barium titanate composite using cultures of human periodontal ligament fibroblasts and keratinocytes. *Acta Biomater* 2010;6:979-89.
  30. Chen C, Wei Y, Jiao X, Chen D. Hydrothermal synthesis of BaTiO<sub>3</sub>: Crystal phase and the Ba<sup>2+</sup> ions leaching behavior in aqueous medium. *Mater Chem Phys* 2008;110:186-91.
  31. Uchino K, Sadanaga E, Hirose T. Dependence of the crystal structure on particle size in barium titanate. *J Am Ceram Soc* 1989;72:1555-8.
  32. Guo HF, Li ZS, Dong SW, Chen WJ, Deng L, Wang YF, et al. Piezoelectric PU/PVDF electrospun scaffolds for wound healing applications. *Colloids Surf B Biointerfaces* 2012;96:29-36.